

Supplementary Information

DNA DAMAGE PHOTO-INDUCED BY CHLOROHARMINE ISOMERS: HYDROLYSIS VERSUS OXIDATION OF NUCLEOBASES

Juan G. Yañuk^a, *M. Paula Denofrio*^a, *Federico A. O. Rasse-Suriani*^{a, b}, *Fernando D. Villarruel*^{a, b},
Federico Fassetta^a, *Fernando S. García Einschlag*^b, *Rosa Erra-Balsells*^c, *Bernd Epe*^d and *Franco*
M. Cabrerizo^{a, *}

^a Instituto de Investigaciones Biotecnológicas - Instituto Tecnológico de Chascomús (IIB-INTECH),
Universidad Nacional de San Martín (UNSAM) - Consejo Nacional de Investigaciones Científicas y
Técnicas (CONICET), Intendente Marino Km 8.2, CC 164 (B7130IWA), Chascomús, Argentina. E-
mail: fcabrerizo@intech.gov.ar

^b INIFTA - CONICET, Universidad Nacional de La Plata, Diag. 113 y 64, (1900) La Plata, Argentina.

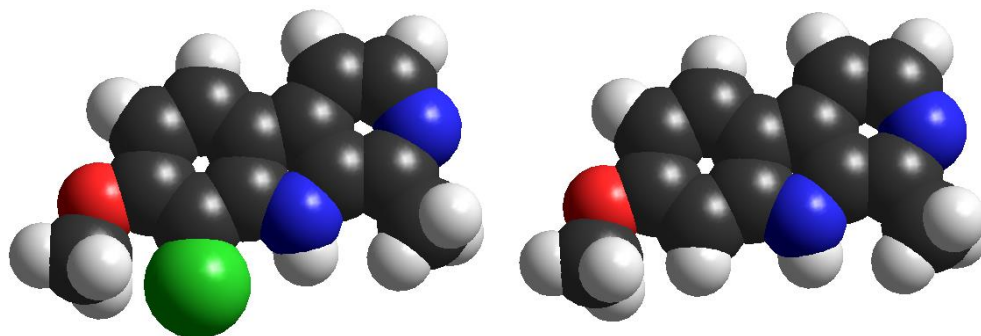
^c CIHIDECAR - CONICET, Departamento de Química Orgánica, Facultad de Ciencias Exactas y
Naturales, Universidad de Buenos Aires, Pabellón 2, 3p, Ciudad Universitaria, (1428) Buenos Aires,
Argentina.

^d Institute of Pharmacy and Biochemistry, University of Mainz, Staudingerweg 5, Mainz, Germany.

* To whom correspondence should be addressed (fcabrerizo@intech.gov.ar)

Contents:	<u>Page</u>
1. Optimized molecule structure of 8-Cl-Ha and Ha	S3
2. Dark controls and time-dependence study of the PM2 damage induced by different concentration of photo-excited 6-Cl-Ha, in phosphate (pH 7.4) buffer	S4
3. Thermal stability of 8-chloroharmine and 6,8-dichloroharmine in phosphate (pH 7.4) buffer solutions	S5
4. SSB modifications induced on DNA by photo-excited Ha, PNS and RB	S6
5. UV-visible absorption spectra of chloroharmines buffered solutions	S7
6. Spectrophotometric titration of 6-Cl-Ha in phosphate buffer solution. MRC-ALS analysis	S8
7. Fluorescence emission spectra of chloroharmines buffered solutions	S9
8. Quenching of fluorescence 8-Cl-Ha by ctDNA	S10
9. Quenching of fluorescence 6,8-diCl-Ha by ctDNA	S11
10. Quenching of fluorescence Ha by ctDNA: Stern-Volmer plot	S12
11. Fluorescence decays and lifetimes of 6-Cl-Ha buffered aqueous solutions	S13
12. Quenching of fluorescence 6-Cl-Ha (pH 7.4) by ctDNA	S14
13. Quenching of fluorescence 6-Cl-Ha (pH 8.1) by ctDNA	S15
14. Multivariate analysis of absorption and fluorescence data obtained for 6-Cl-Ha	S16
15. Normalized damage profile induced by 6-Cl-Ha under different pH conditions	S18
16. Damage profile induced by 6-Cl-Ha at pH 8.1, in the presence of isopropanol	S19
17. Time-dependence study of the SSBs and Fpg-sensitive base modifications photoinduced by 6-Cl-Ha (20 μ M) in phosphate buffer solution pH 8.1 and 8.7	S20
18. Effect of isopropanol and L-histidine on 6-Cl-Ha (pH 8.1) UV-visible absorption and fluorescence emission spectra	S21

1. Optimized molecule structure of 8-Cl-Ha and Ha



Scheme SI.1. Optimized molecule structure of 8-Cl-Ha (left) and Ha (right).

Molecular Modeling.

The ground-state geometry of Ha and 8-Cl-Ha were calculated by using the semiempirical parametrized PM3 method as implemented in version of the HyperChem Professional for Windows program (Restricted Hartree-Fock (RHF) formalism; total charge: 0; spin multiplicity: 1; convergence limit: 1e-008; iteration limit: 50; accelerate convergence: on; CI method: none; Polak-Ribiere algorithm; RMS gradient: 0.006 kcal/(Å mol); in vacuo). PM3 has proved to be effective in studies on aromatic molecules containing heteroatoms, compared with other methods such as MINDO/3 or MNDO.

2. Dark controls and time-dependence study of the PM2 damage induced by different concentration of photo-excited 6-Cl-Ha, in phosphate (pH 7.4) buffer solutions

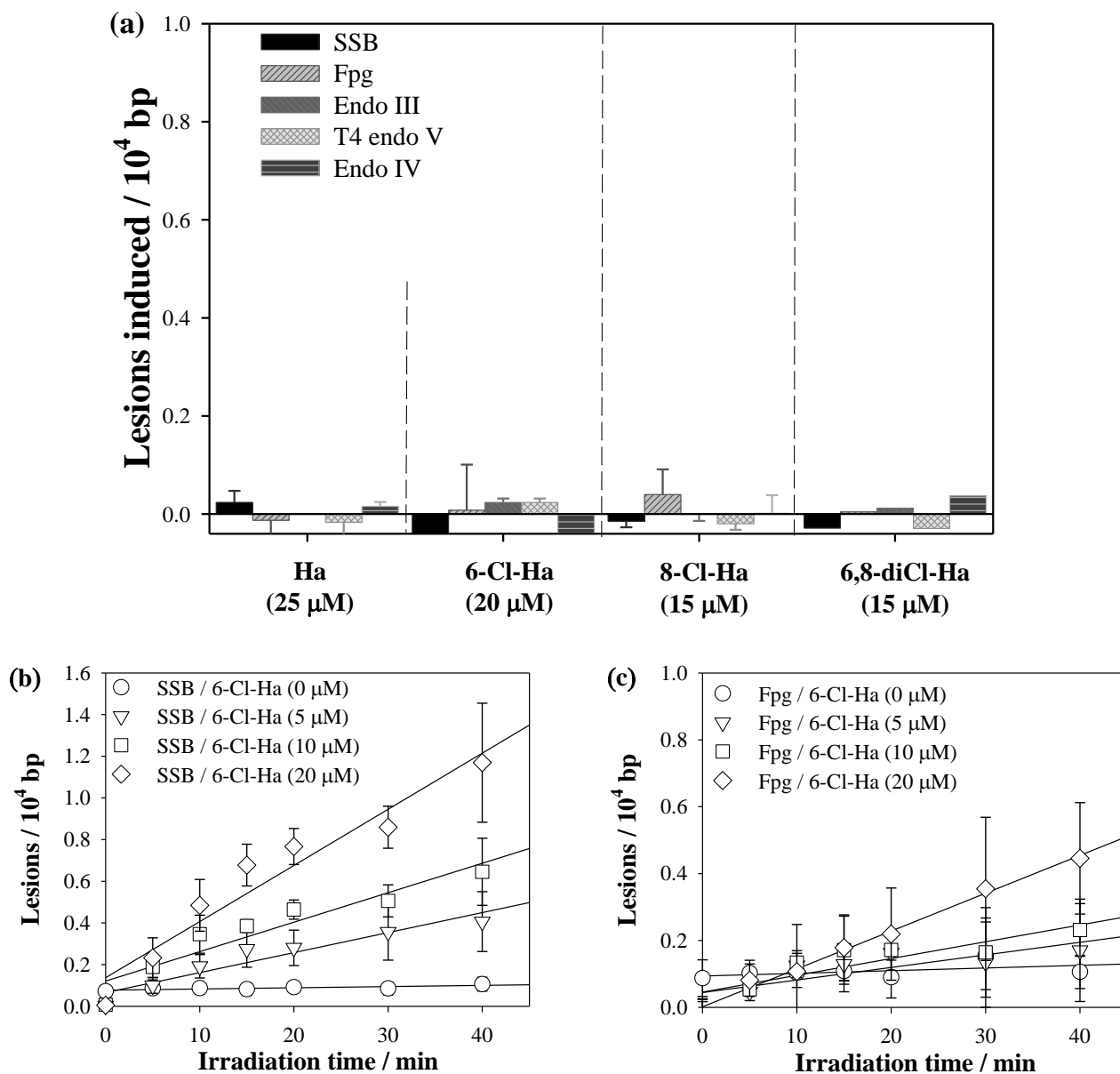


Figure SI.1. (a) DNA damage induced by the maximum concentration of the three chloroharmines used (*dark controls*). (b) and (c) time-dependence of SSBs and Fpg-sensitive sites modifications, respectively, induced by 6-Cl-Ha (0 μM, 5 μM, 10 μM and 20 μM). Data are the means of 4 independent experiments (\pm S.D).

3. Thermal stability of 8-chloroharmine and 6,8-dichloroharmine, in phosphate (pH 7.4) buffer solutions

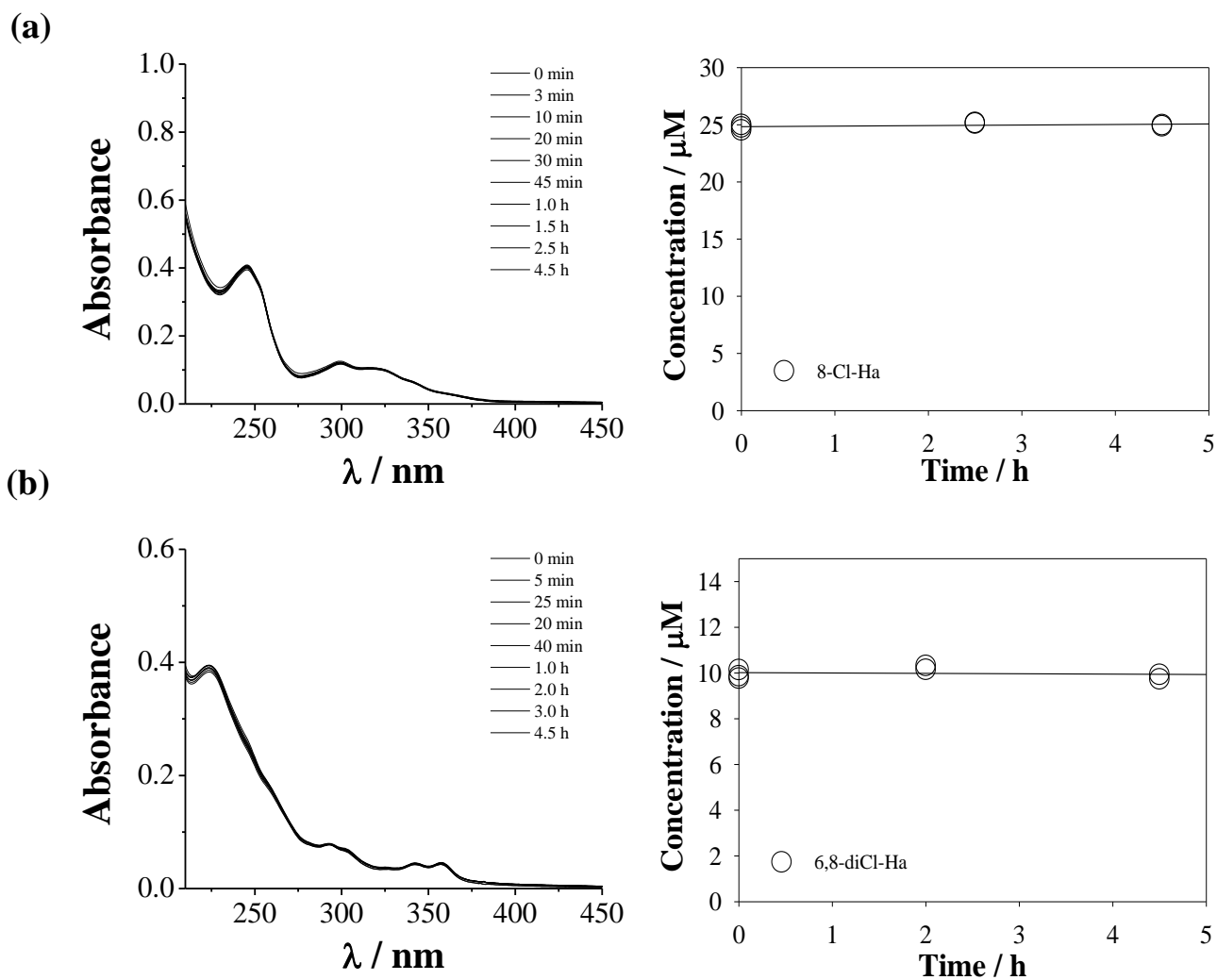


Figure SI.2. UV-vis absorption spectra (*left column*) and HPLC analysis (*right column*) of (a) 8-chloroharmine and (b) 6,8-dichloroharmine phosphate buffer solutions (pH 7.4) kept in the dark for 4.5 h.

4. SSB modifications induced on DNA by photo-excited Ha, PNS and RB

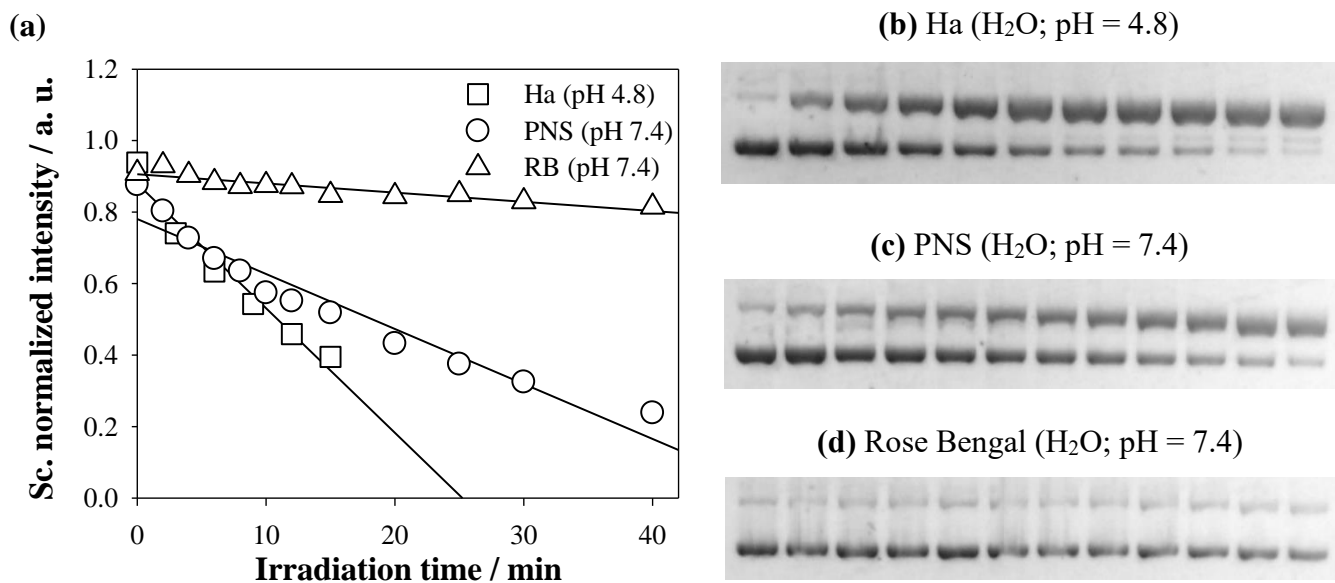


Figure SI.3. (a) Evolution of the normalized intensity of the pGEM-3z Sc form as a function of irradiation time. Experiments were performed in plasmid DNA (pGEM-3z) air-equilibrated aqueous solution, in the presence of Ha, perinaphthenone-2-sulfonic acid (PNS) and Rose Bengal (RB). (b), (c) and (d) show the corresponding agarose gel. For comparative reasons, the absorbance of the photosensitizer solutions was matched at the excitation wavelength (*i.e.*, $A^{350\text{nm}} = 0.3$).

5. UV-visible absorption spectra of chloroharmines buffered solutions

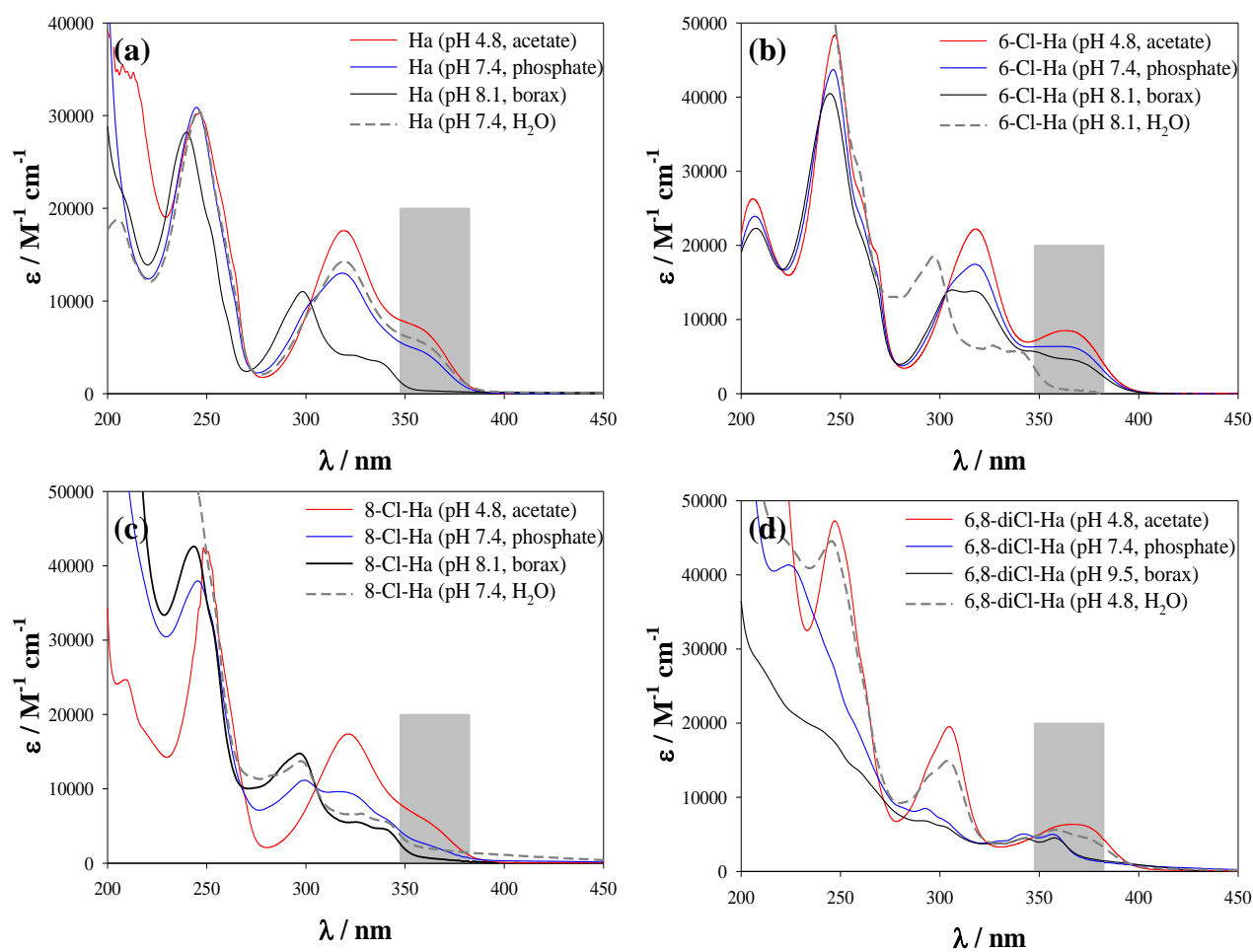


Figure SI.4. UV-vis absorption spectra of aerated aqueous (grey-dashed line) and buffered (solid lines) solutions of (a) Ha, (b) 6-Cl-Ha, (c) 8-Cl-Ha and (d) 6,8-diCl-Ha. Grey bar depicts the irradiation range used in this work ($365 \pm 20 \text{ nm}$).

6. Spectrophotometric titration of 6-Cl-Ha in phosphate buffer solution. MRC-ALS analysis

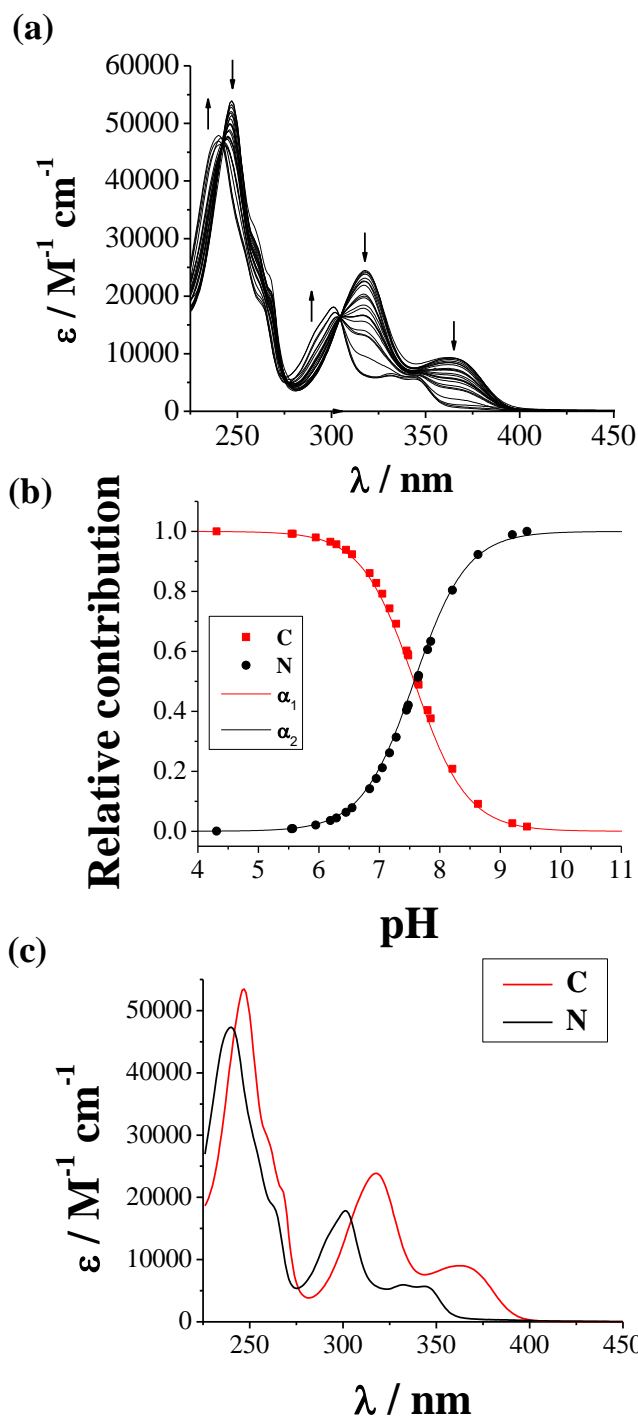


Figure SI.5. (a) UV-visible absorption spectra vs pH (arrows indicate the changes in band intensities as the pH increases) (b) Distribution functions obtained for cationic (C) and neutral (N) species of 6-Cl-Ha by the MCR-ALS hybrid (hard-soft) modelling methodology [1-5] (c) Optimized molar absorptivity of the deconvoluted species.

References:

1. F. A. O. Rasse-Suriani, F. S. García-Einschlag, M. Rafti, T. S. D. León, P. M. David Gara, R. Erra-Balsells and F. M. Cabrerizo, *Photochemistry and Photobiology*, 2017, DOI: 10.1111/php.12811, n/a-n/a.
2. Jaumot, J., R. Eritja and R. Gargallo, *Anal. Bioanal. Chem.*, 2011, **399**, 1983–1997.
3. A. de Juan, R. Gargallo, J. Jaumot and R. Tauler, *Chemometrics and Intelligent Laboratory Systems*, 2005, **76**, 101-110.
4. A. de Juan and R. Tauler, *Analytica Chimica Acta*, 2003, **500**, 195-210.
5. P. J. Gemperline and E. Cash, *Analytical Chemistry*, 2003, **75**, 4236-4243.

7. Fluorescence emission spectra of chloroharmines buffered solutions

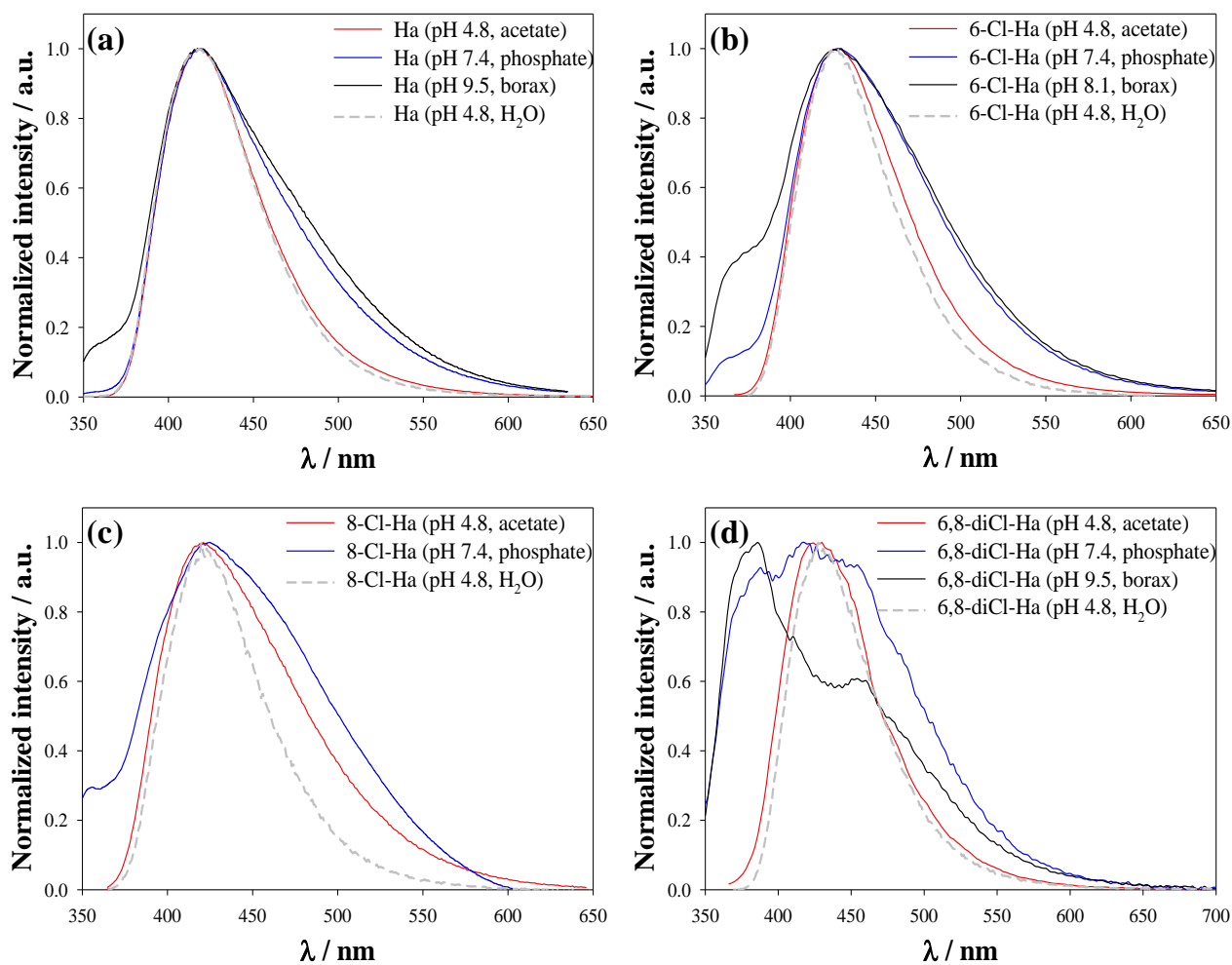


Figure SI.6. Normalized fluorescence emission spectra ($\lambda_{\text{exc}} = 340$ nm) of aerated aqueous (grey-dashed lines) and buffered (solid lines) solutions of (a) Ha, (b) 6-Cl-Ha, (c) 8-Cl-Ha and (d) 6,8-diCl-Ha.

8. Quenching of fluorescence 8-Cl-Ha by ctDNA

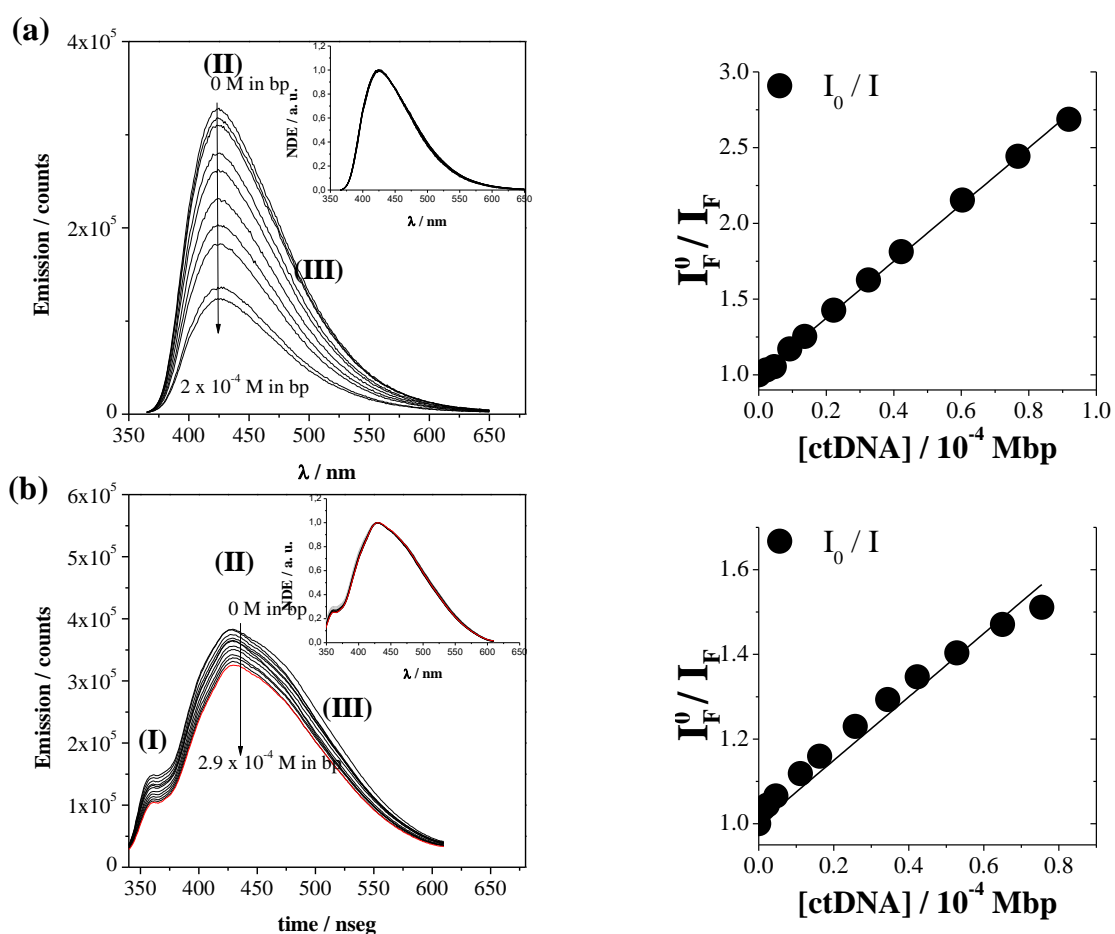


Figure SI.7. Steady-state fluorescence emission of 8-Cl-Ha buffered solution (15 μ M) recorded in the presence of increasing amounts of ctDNA: **(a)** pH 4.8 ($\lambda_{exc} = 360$ nm) and **(b)** pH 7.4 ($\lambda_{exc} = 340$ nm). *Left column:* corrected fluorescence emission spectra. Arrows indicate the variation in ctDNA concentration (Mbp). (I), (II) and (III) correspond to the emission bands of neutral protonated and zwitterionic species of 8-Cl-Ha, respectively. *Insets in left column:* Normalized Emission (NE) spectra. *Right column:* Stern–Volmer plots of the fluorescence intensities (I_F). I_F was calculated as the integral below the whole emission spectra.

9. Quenching of fluorescence 6,8-diCl-Ha by ctDNA

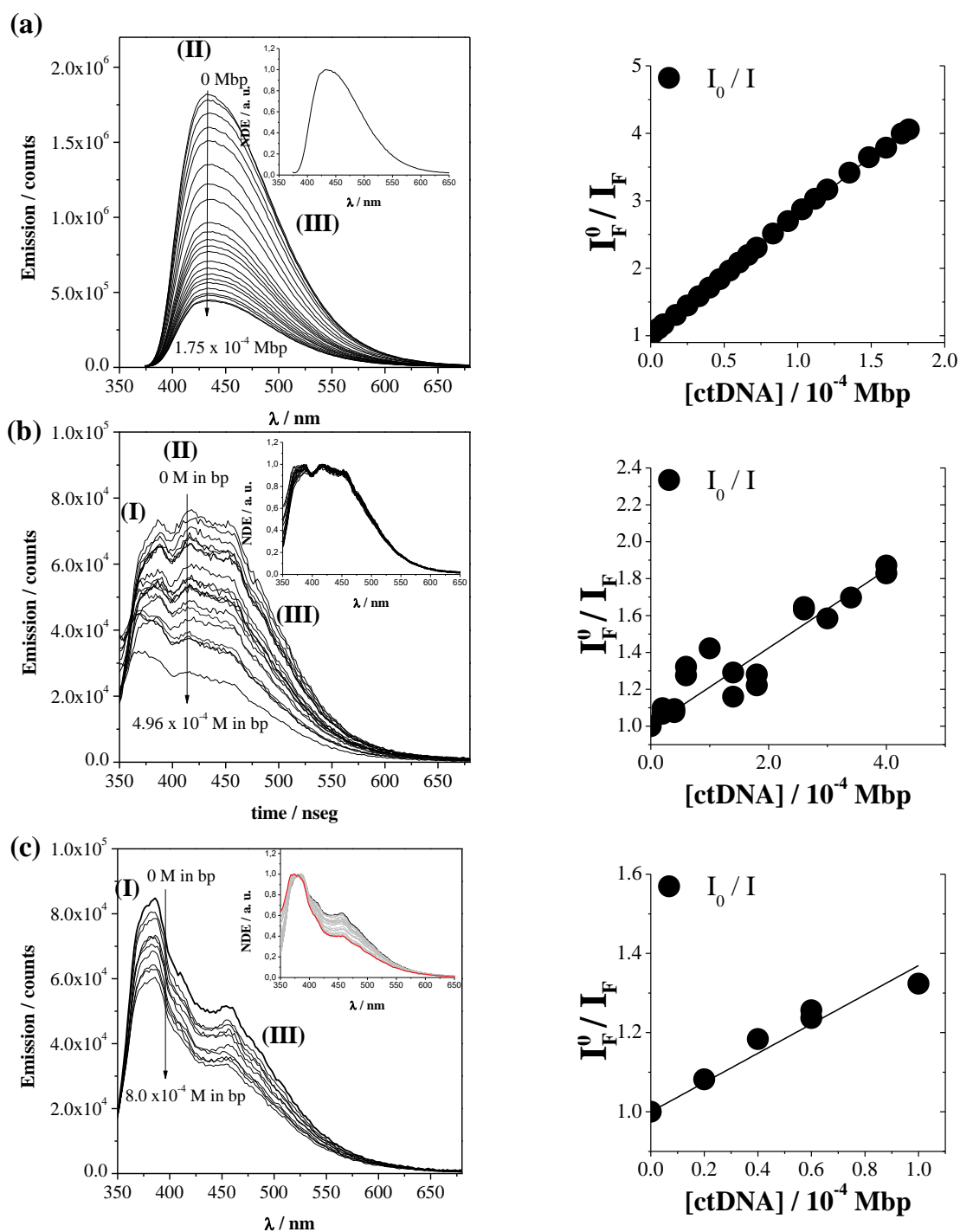


Figure SI.8. Steady-state fluorescence emission of 6,8-diCl-Ha buffered solution ($11.5 \mu\text{M}$) recorded in the presence of increasing amounts of ctDNA: (a) pH 4.8 ($\lambda_{\text{exc}} = 368 \text{ nm}$), (b) pH 7.4 ($\lambda_{\text{exc}} = 345 \text{ nm}$) and (c) pH 8.1 ($\lambda_{\text{exc}} = 345 \text{ nm}$). *Left column:* corrected fluorescence emission spectra. Arrows indicate the variation in ctDNA concentration (Mbp). (I), (II) and (III) correspond to the emission bands of neutral protonated and zwitterionic species of 6,8-diCl-Ha, respectively. *Insets in left column:* Normalized Emission (NE) spectra. *Right column:* Stern–Volmer plots of the fluorescence intensities (I_F). I_F was calculated as the integral below the whole emission spectra.

10. Quenching of fluorescence Ha by ctDNA: Stern-Volmer plot

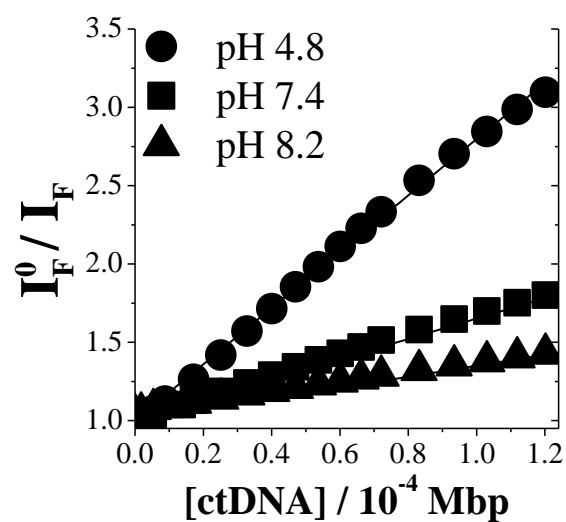


Figure SI.9. Stern–Volmer plots of the fluorescence intensities (I_F) of Ha buffered solution ($12 \mu\text{M}$) emission recorded in the presence of increasing amounts of ctDNA, under different pH conditions. I_F was calculated as the integral below the whole emission spectra.

11. Fluorescence decays and lifetimes of 6-Cl-Ha buffered aqueous solutions

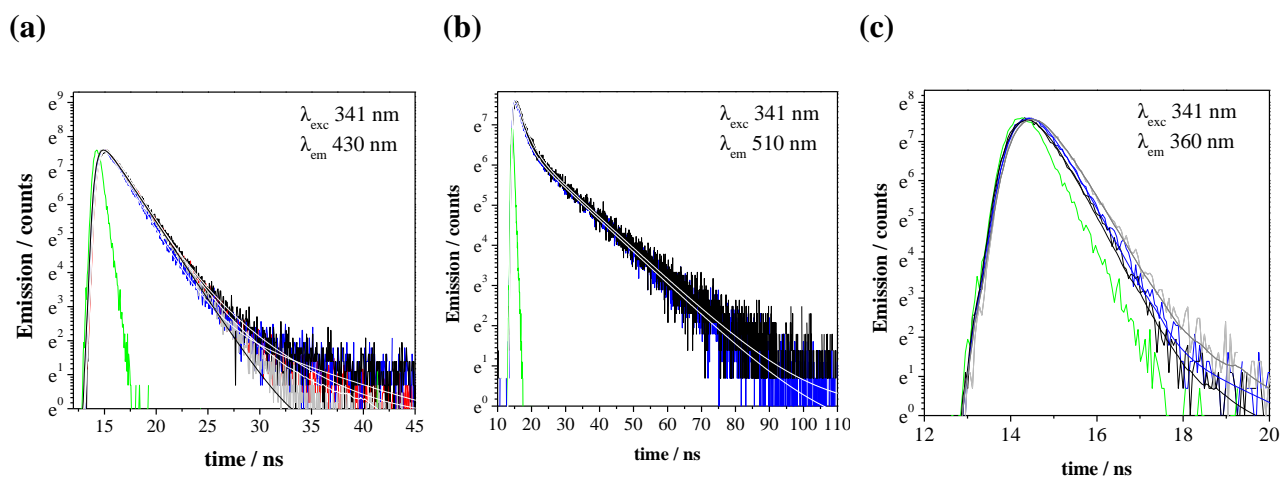


Figure SI.10. Fluorescence decays of 6-Cl-Ha (20 μ M) recorded in aerated buffered aqueous solutions at different pH values: acetate pH 4.8 (red line), phosphate pH 7.4 (blue line) and borax pH 8.1 (black line). Green and white lines represent prompt signal and bi-exponential fit. $\lambda_{exc} = 341$ nm and $\lambda_{em} = 430$ nm (a), 510 nm (b) and 360 nm (c).

Table SI.1. Lifetime values (τ) determined under three different pH conditions (*i.e.*, 4.8, 7.4 and 8.1) from decays recorded under three different emission wavelengths (*i.e.*, 360 nm, 430 nm and 510 nm).

pH condition (buffer)	λ_{em} / nm	τ_C / ns	$\langle\tau_C\rangle$ / ns	τ_N / ns	$\langle\tau_N\rangle$ / ns	τ_Z / ns	$\langle\tau_Z\rangle$ / ns		
4.8 (acetate)	430	2.10	2.0 ± 0.1	Nd	---	12.1	12.0 ± 0.2		
	7.4 (phosphate)	360		1.97		0.34		nd	11.0 ± 1
		430		1.93		Nd		0.2	
	510	1.98	Nd		12.6				
8.1 (borax)	360	1.97	2.2 ± 0.1	0.29	$0.4 \pm$	nd	12.4 ± 0.4		
		430		2.17		Nd		0.2	12.1
		510		2.35		Nd			12.8

12. Quenching of fluorescence 6-Cl-Ha (pH 7.4) by ctDNA

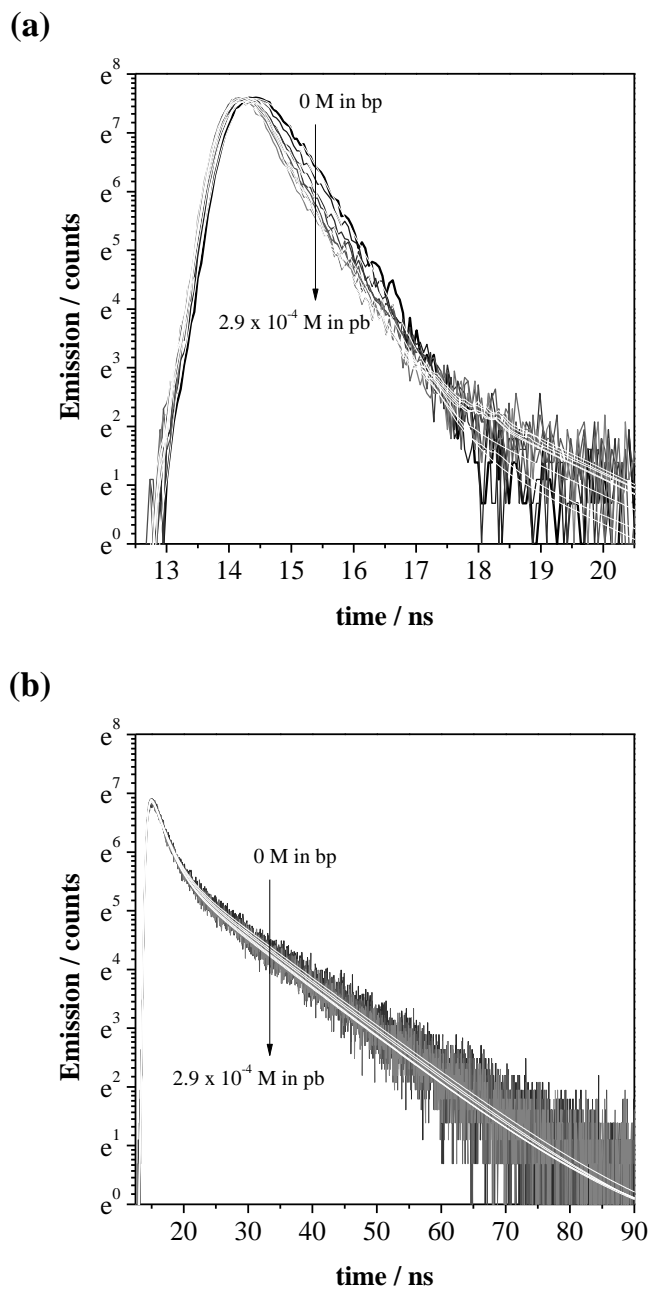


Figure SI.11. Fluorescence emission decays of 6-Cl-Ha phosphate buffer solution ($20\ \mu\text{M}$, pH 7.4) recorded in the absence and in the presence of increasing amounts of ctDNA. Arrows indicate the variation in ctDNA concentration (Mbp). **(a)** ($\lambda_{\text{exc}} = 341\ \text{nm}$ and $\lambda_{\text{em}} = 360\ \text{nm}$) **(b)** ($\lambda_{\text{exc}} = 341\ \text{nm}$ and $\lambda_{\text{em}} = 510\ \text{nm}$).

13. Quenching of fluorescence 6-Cl-Ha (pH 8.1) by ctDNA

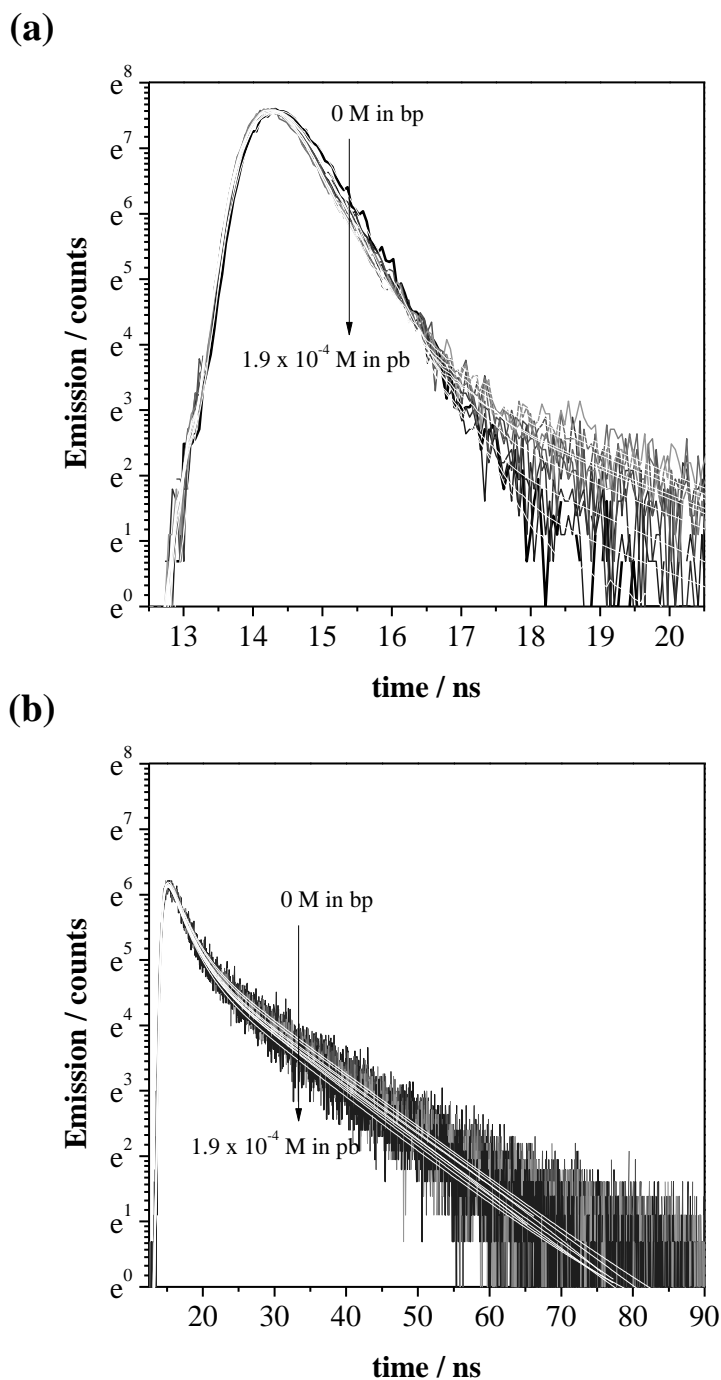


Figure SI.12. Fluorescence emission decays of 6-Cl-Ha borax buffer solution (20 μ M, pH 8.1) recorded in the absence and in the presence of increasing amounts of ctDNA. Arrows indicate the variation in ctDNA concentration (Mbp). **(a)** ($\lambda_{\text{exc}} = 341$ nm and $\lambda_{\text{em}} = 360$ nm) **(b)** ($\lambda_{\text{exc}} = 341$ nm and $\lambda_{\text{em}} = 510$ nm).

14. Multivariate analysis of absorption and fluorescence data obtained for 6-Cl-Ha

The distinctive spectroscopic behaviour of 6-Cl-Ha observed in the presence of ctDNA was further analysed by multivariate analysis of absorption and fluorescence data. Three different types of data matrices (D_{Em} , D_{Ab} and D_{Ex}) were constructed by collecting the emission, absorption and excitation spectra of 6-Cl-Ha solutions under different experimental conditions (pH and [ctDNA]).

Emission Spectra. In order to retrieve the spectral contributions associated to the emissions from the excited states of 6-Cl-Ha in phosphate buffer solutions in the absence of DNA, a curve resolution procedure was applied to the 2-way augmented array $D_{Em}(i \times j)$ constructed by stacking all the emission spectra obtained at different excitation wavelengths and pH conditions. Briefly, singular value decomposition (SVD) suggested that D_{Em} , containing the whole set of emission spectra obtained at different excitation wavelengths ranging from 300 to 450 nm and pH values ranging from 6.2 to 9.4, can be properly described by four independent contributions. A further bilinear analysis of D_{Em} by the MCR-ALS algorithm allowed us to retrieve the underlying emission spectra (Figure 5a, main text) with an overall lack of fit (LOF) of less than 0.7 %. Comparison of the latter emission spectra with those previously reported for nHo [1] suggests that spectral contributions resolved for 6-Cl-Ha may be ascribed to N^* , C^* , A^* and Z^* , respectively. Noteworthy, despite the MCR-ALS analysis of D_{Em} unveiled the contribution of a fourth species to the spectra shown in Figure 5b (main text), the contribution ascribed to A^* is rather low (*i.e.*, < 5.5% for the entire sample set), and practically independent of the sample pH (data not shown). The presence of A^* is also confirmed by the analysis of D_{Ex} (*vide infra*).

In addition, the analysis of fluorescence data obtained in the presence of different [ctDNA] shows that $D_{Em,DNA}$ matrix (containing the whole set of emission spectra obtained at different excitation wavelengths, pH buffer condition 7.2 and 8.1, and [ctDNA]) can also be properly described by the spectral contributions shown in Figure 5a (main text), suggesting that the nature of the emitting species is not affected by the presence of ctDNA.

Absorption Spectra. A multivariate analysis was performed on the 2-way augmented array constructed by stacking the entire set of absorbance spectra obtained for 6-Cl-Ha phosphate buffer solutions at different pH values and [ctDNA] (*i.e.*, $D_{Ab,DNA}$). Singular value decomposition (SVD) suggested only two contributions for the subset of spectra obtained during 6-Cl-Ha pH-titration in the absence of ctDNA (D_{Ab}), whereas three independent contributions (Figure 5b, main text) were required in order to properly describe $D_{Ab,DNA}$. Noteworthy, the additional contribution observed in the presence of ctDNA, which resembles the spectrum of C although somewhat red shifted, exhibits important absorptions at wavelengths where ctDNA absorption can be considered negligible. Moreover, for the two pH conditions tested (phosphate buffers of pH 7.2 and 8.1), the spectral contribution of the additional species increases with [ctDNA] (Figure SI.13a) thus providing a strong

evidence of the formation of a ground state complex between the cationic species of 6-Cl-Ha (C) and ctDNA.

Excitation Spectra. A similar procedure was applied to the excitation spectra obtained under different experimental conditions (*i.e.*, emission wavelengths, pH value and [ctDNA]). Two excitation matrices D_{Ex} and $D_{\text{Ex,DNA}}$ were constructed from the spectra recorded in the absence (*i.e.*, pH-titration) and in the presence of increasing amounts of ctDNA, respectively. The analysis of singular values suggested three and four independent contributions for describing the spectra of D_{Ex} and $D_{\text{Ex,DNA}}$, respectively. The application of MCR-ALS algorithm to both D_{Ex} and $D_{\text{Ex,DNA}}$ yielded the excitation spectra shown in Figure 5c (main text), the contribution labelled as “static complex” being only necessary for describing those excitation spectra recorded in 6-Cl-Ha solutions with added ctDNA (*i.e.*, $D_{\text{Ex,DNA}}$).

The excitation spectra obtained for N^* and C^* closely match the absorption spectra shown in Figure 5b (main text). In addition, the additional spectral shape (in green) required to describe the excitation spectra in the presence of ctDNA correlates well with the absorption spectrum ascribed to the “static complex”. Interestingly, in line with the results obtained from the analysis of the emission spectra, an additional contribution is required to describe the fluorescence results even in the absence of ctDNA. The excitation spectra associated to this additional contribution supports the previous assumption regarding the contribution of A^* species to the observed fluorescence spectra. It is worth noting that, as previously stated, the latter contribution is rather small, almost independent of the solution pH and can only be evidenced from a detailed analysis of the entire range of excitation and emission wavelengths.

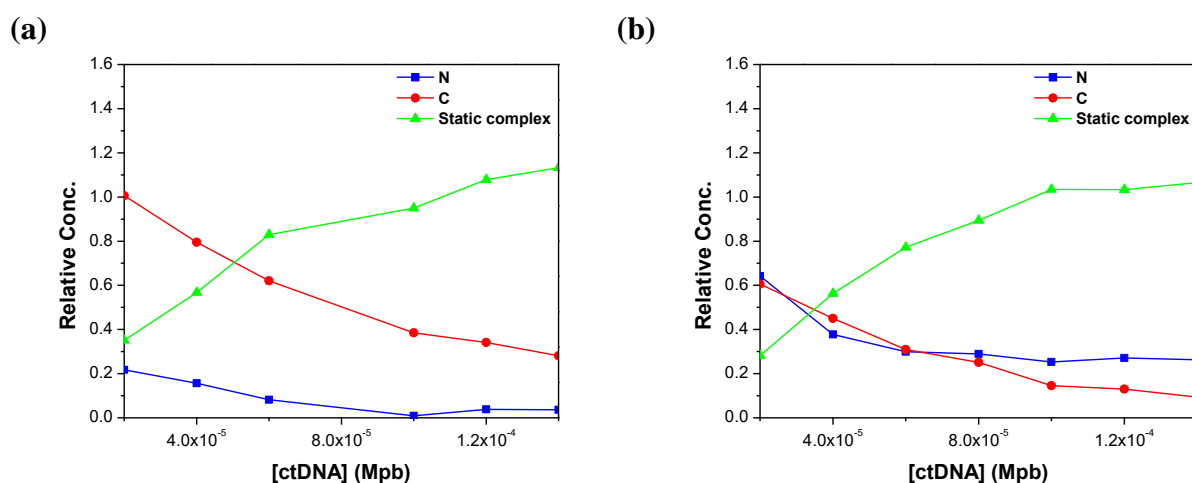


Figure SI.13. Evolution of relative concentration of each deconvoluted spectra obtained with multivariate analysis of absorbance arrays of 6-Cl-Ha in phosphate buffer with increasing amounts of ctDNA at pH 7.2 (a) and pH 8.1 (b).

Reference:

[1] F. A. O. Rasse-Suriani, F. S. García-Einschlag, M. Rafti, T. S. D. León, P. M. David Gara, R. Erra-Balsells and F. M. Cabrerizo, *Photochemistry and Photobiology*, 2018, **94**, 36-51.

15. Normalized damage profile induced by 6-Cl-Ha under different pH conditions

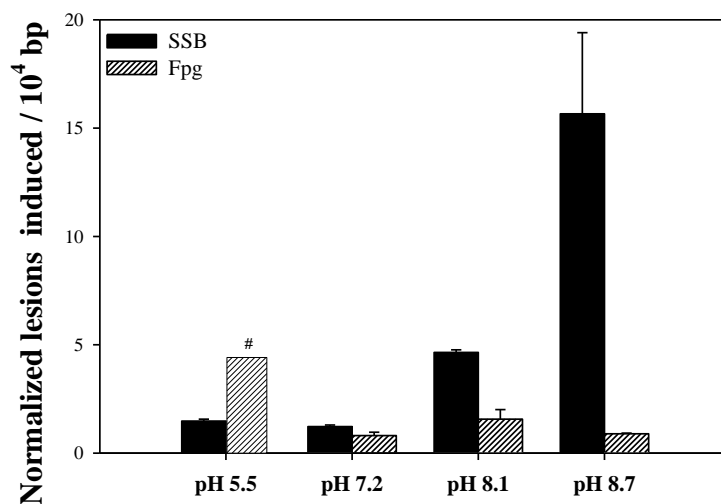


Figure SI.14. Normalized SSB and Fpg-sensitive modifications induced in PM2 DNA by photo-excited 6-Cl-Ha ($A^{366\text{nm}} = 0.12$) exposure to 20 min of UVA light ($365 (\pm 20)$ nm) in aqueous solution under different pH conditions. # indicates data out of range. In all the cases, data are the means of 3 independent experiments (\pm S.D).

16. Damage profile induced by 6-Cl-Ha at pH 8.1, in the presence of isopropanol

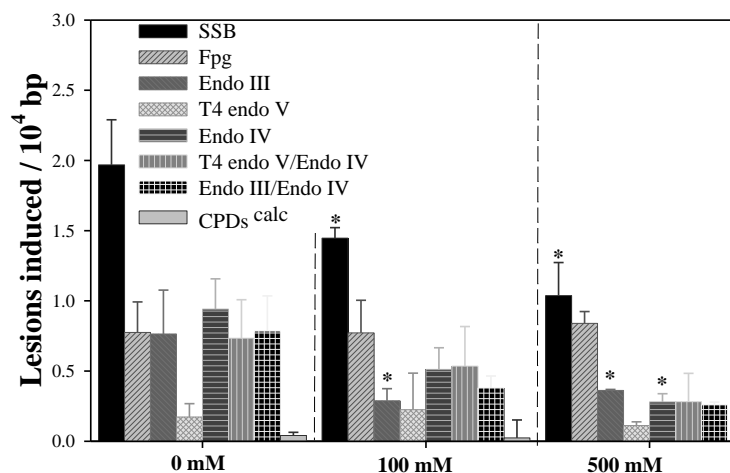
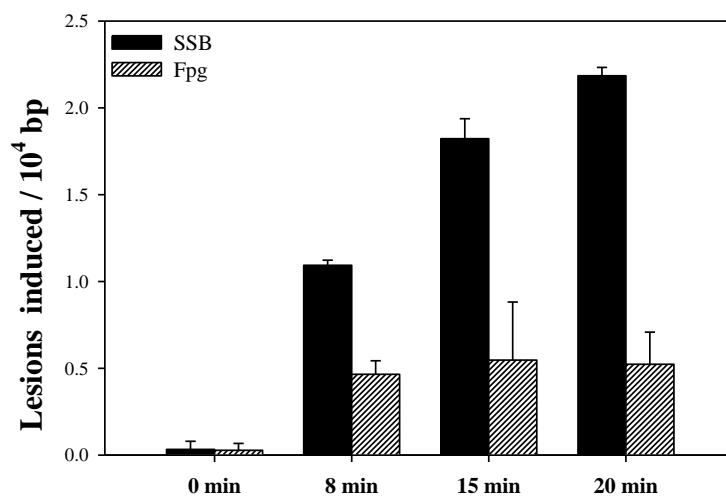


Figure SI.15. DNA damage profile showing SSB and several endonuclease sensitive modifications induced in PM2 DNA by photo-excited (UVA 365 (\pm 20) nm, 20 min) 6-Cl-Ha (20 μ M, in phosphate buffer, at pH 8.1) in the presence of three different concentrations of isopropanol (0 mM, 100 mM and 500 mM). In all the cases, data are the means of 3 independent experiments (\pm S.D). * indicates statistically significant differences in each DNA modifications between samples irradiated in the presence of isopropanol and their corresponding controls (*i.e.*, isopropanol 0 mM) ($p < 0.05$, ANOVA / Dunnett's tests).

17. Time-dependence study of the SSBs and Fpg-sensitive base modifications photoinduced by 6-Cl-Ha (20 μ M) in phosphate buffer solution pH 8.1 and 8.7

(a)



(b)

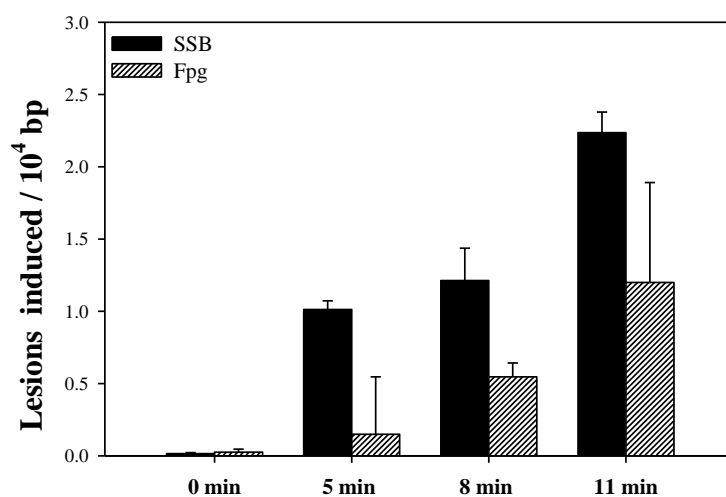


Figure SI.16. SSB and modifications sensitive to Fpg protein induced in PM2 DNA by exposure to UVA light (365 (\pm 20) nm) at different irradiation time in the presence of 20 μ M of 6-chloroharmine in phosphate buffer at (a) pH 8.1 and (b) pH 8.7. Data are the means of 3 independent experiments (\pm S.D).

18. Effect of isopropanol and L-histidine on 6-Cl-Ha (pH 8.1) UV-visible absorption and fluorescence emission spectra

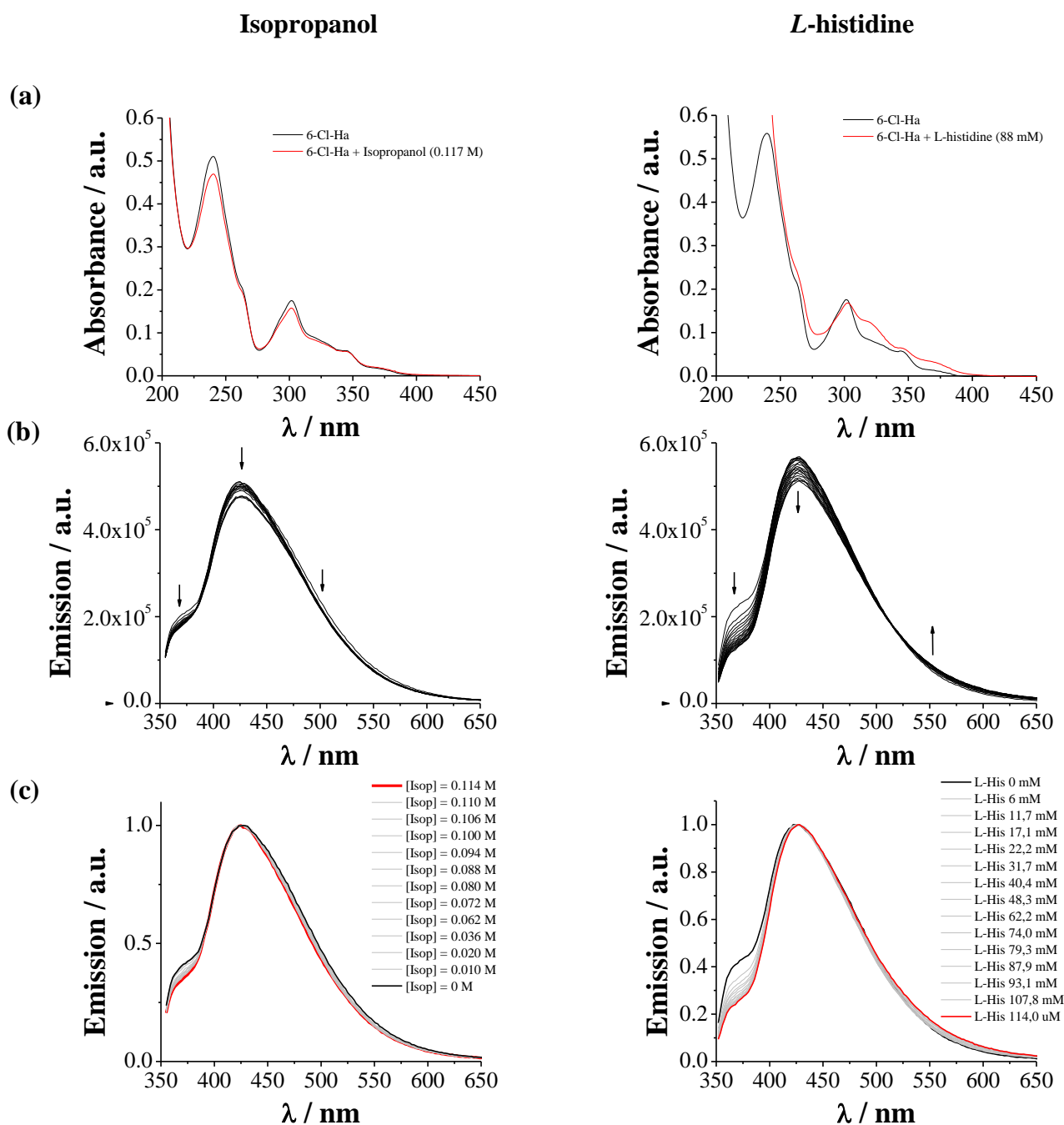


Figure SI.17. UV-visible absorption (a) and emission (b) and normalized emission (c) spectra of 6-Cl-Ha buffer solution (pH 8.1) recorded in the presence of increasing amount of isopropanol (*left column*) and L-histidine (*right column*).